This is the pre-review version of the paper published in

J. Phys. Chem. A, 122, 7497-7507

The final version of this paper is available through the American Chemical Society website in

https://dx.doi.org/10.1021/acs.jpca.8b06894

The influence of alkyne and azide substituents on the choice of the reaction mechanism of the Cu^+-catalyzed addition of azides to iodoalkynes

Pedro J. Silva* and Carlos E.P Bernardo

FP-ENAS/ Fac. de Ciências da Saúde, Univ. Fernando Pessoa, Rua Carlos da Maia, 296, 4200-150 Porto-Portugal. *pedros@ufp.edu.pt

Abstract

The cycloaddition of azides to iodoalkynes is strongly enhanced by some Cu^+-complexes. We have studied computationally six reaction pathways for the cycloaddition of twenty-four combinations of azide and iodoalkyne to identify the dominant pathways and the influence of reactant structure on the evolution of the reaction. Two pathways were found to be operating for distinct sets of reactants. In the first pathway, initial complexation of iodoalkyne by Cu^+ is followed by the binding of the azide to bind to the metal through its substituted nitrogen atom, followed by attack of the non-halogenated alkyne carbon by the terminal nitrogen atom. This pathway is generally followed by aromatic or electron-deficient azides, unless the iodoalkyne bears an electron-withdrawing group. The second pathway is a single-step mechanism similar (apart from the alkyne bond weakening caused by complexation) to that observed in the absence of catalyst. Electron-deficient iodoalkynes and methyl azides strongly prefer this mechanism, regardless of the identity of thie reaction partners. The catalytic gain obtained through the use of Cu^+ depends only partially on its direct effect on the energy of the transition state (relative to that of the infinitely separated reactants) and may be lost if the iodoalkyne itself strongly interacts with the catalyst through the formation of too strong a π-complex.

Introduction

Fast, selective and sterospecific organic reactions between simple building blocks are commonly labeled "click chemistry"[1]. Click reactions can be divided into four main categories: (i) cycloaddition of 1,3-dipolar unsaturated species[2] (ii) nucleophilic substitution chemistry on strained ring systems[1] (iii) reactions involving non-aldol type carbonyl chemistry[1,3,4] and (iv) addition reactions to carbon-carbon multiple bonds[5–8], and have found wide applicability also in materials science, medicinal chemistry and biopolymers[9]. The classical example of a click reaction is a modification of the original Huisgen 1,3-dipolar cycloaddition between azides and alkynes, which gives 1,2,3-triazoles as a mixture of 1,4- and

1,5-substituted regioisomers [2]. This [3+2] azide-alkyne cycloaddition proceeds slowly in the absence of a catalyst and usually requires high temperatures. In 2002, Sharpless, Kolb and Tornøe independently applied Cu^{+} as a catalyst in the original Huisgen reaction, making it fast and accessible at room temperature and pressure[10–12]. The Cu(I) catalyst appreciably lowers the activation barrier, and confers selectivity to the reaction, which then yields only the 1,4-isomeric product. The reaction has been renamed as "copper-catalyzed azide/alkyne cycloaddition" (CuAAC) and is characterized by its orthogonality, versatility, fidelity,and regioselectivity. This reaction is however only accessible to terminal alkynes, which limits its use in the synthesis of other substituted triazoles.

The mechanism of this reaction has been extensively investigated by experimental and computation methods[13–25]. Copper (I) was initially proposed[13] to bind to the alkyne, increasing its acidity and facilitating its deprotonation. The substituted azide would then attack the Cu atom in the Cu^{+}-acetylide complex through its substituent-proximal nitrogen atom. Electronic rearrangement of the π-electrons would close the ring, yielding a six-membered metallacyclic structure. As the ring rearranges into a five-membered triazole, the Cu atom would be released from the nitrogen atom while still binding to the carbon atom from the original acetylenic moiety. Finally, protonation of this carbon would cleave the carbon-copper bond and release the Cu catalyst[13].

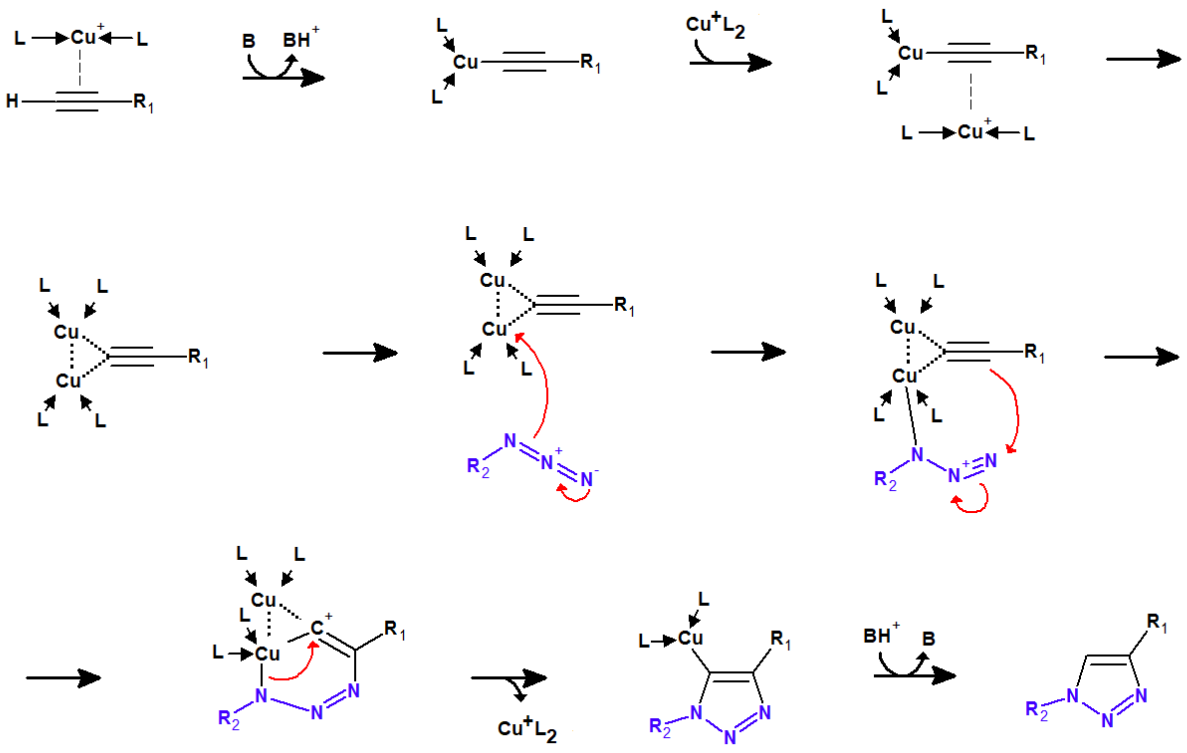

Figure 1. Reaction mechanism of the Cu^{+}-catalyzed addition of azides to terminal alkynes[15,22]

The subsequent finding of second-order kinetics relative to the catalyst[26,27] and experimental evidence for binuclear reaction intermediates[16,18] prompted the modification of this mechanism to include simultaneous intervention of two (or more) Cu^+ ions as acetylide-Cu^+ complexes and azide-activating catalyst[15,22] (Figure 1).

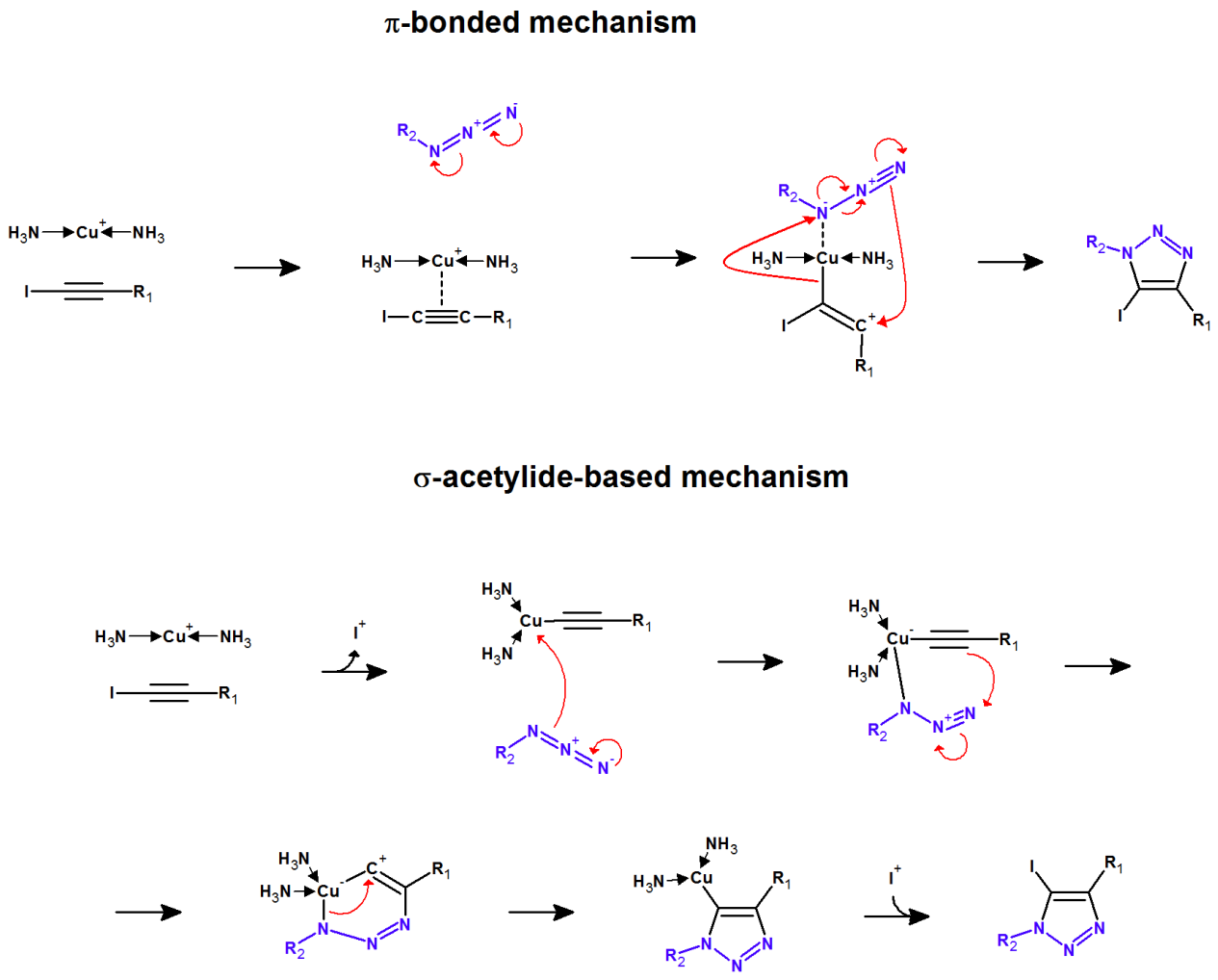

Figure 2: Proposed reaction mechanisms for the Cu+-catalyzed coupling of azides to iodoalkynes[28]

In an effort to enhance the scope of this useful reaction, Hein *et al.*[28] reported that reactions between substituted iodoalkynes and organic azides yield 5-iodo-1,4,5-triazoles which cannot otherwise be produced using a CuAAC. This reaction is especially attractive because iodoalkynes are stable and very readily accessible, which allows the facile synthesis of many different substituted 1,4,5-triazoles. As iodoalkynes do not have an acidic acetylenic proton, the reaction mechanism in this instance is most likely to differ from that described by Himo and co-workers[13], and therefore Hein *et al.* suggested two reaction

pathways differing among themselves on the Cu^+-binding mode to the iodoalkyne (either σ- or π-) that would involve the coordination of azide to the Cu^+ ion as the regio-controlling step[28] (Figure 2).

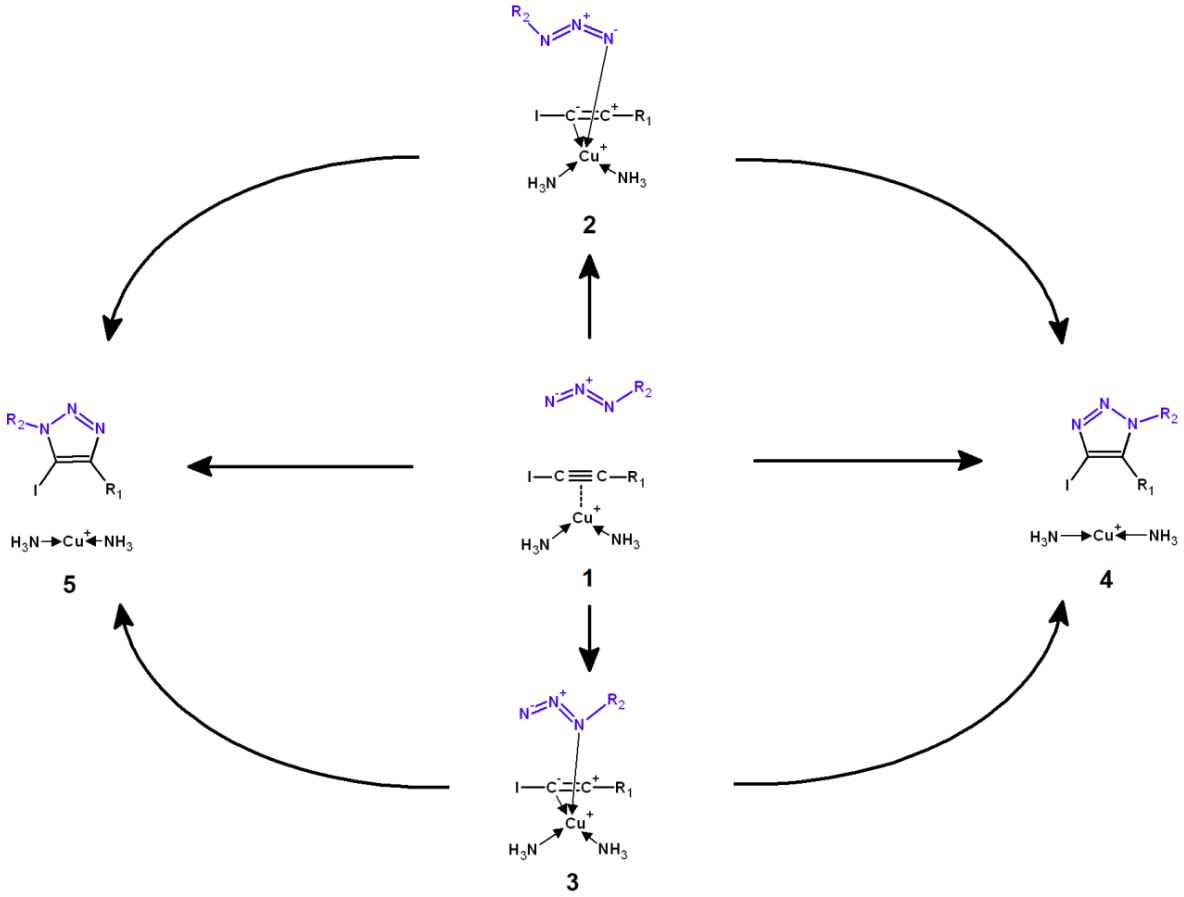

Figure 3: The six reaction pathways arising from azide addition to π-complexed iodoalkynes.

Their experimental results disfavored the pathway that relied on σ-bonding of Cu^+ to iodoalkyne and subsequent loss of iodine, as no evidence for the formation of iodine-free products was found, even in the presence of polar solvents or reagents bearing acidic protons[28]. NMR-tracking of the reaction of azides with 1-iodoalkynes produced *in situ* from alkyne and lithium iodide later showed that iodine-free triazole could only be produced after 1-iodoalkyne was fully spent, further confirming that pathways involving de-iodination of the 1-iodoalkynes are not operating at measureable rates[29]. Computational studies on the addition of benzyl azide to 1-iodo(ethynylbenzene) by Lal *et al.*[30] have further shown that a variant of the σ-acetylide-based mechanism entailing oxidative addition of the carbon iodide to the Cu^+-based catalyst (yielding a formal oxidation of Cu^+ to Cu^{3+}) can also be ruled out due to activation energies in excess of 40 kcal·mol^{-1}. In that important work, the activation energy of the single-step addition of azide to the Cu^+-complexed iodoalkyne (Figure 3, pathway 1→5) was shown to be very similar to that of the mechanism involving Cu^+ attack by the substituted azide nitrogen and subsequent addition of the terminal azide

nitrogen to the non-halogenated alkyne carbon (Figure 3, pathway 1→3→5). The Cu^+-complex was also found to dramatically lower the activation barrier by 10 kcal·mol^{-1} (in pathway 1→5) or 12 kcal·mol^{-1} (pathway 1→3→5) compared to the uncatalyzed reaction.

Since the presence of mechanisms with similar barriers raises the intriguing possibility of tuning the choice of reaction mechanism by changing the nature of the substituents on the iodoalkyne and/or azide, we have decided to study the six possible reaction pathways (yielding either 4-iodo-1,2,3-triazoles or 5-iodo-1,2,3-triazoles) for twenty-four combinations of starting materials. We compute the catalytic effect of the Cu^+-complex to be at most 6.3 kcal.mol^{-1} , i.e. about half of the dramatic estimates reported by Lal *et al.*[30] due to their use of infinitely separated reactants (rather than the more stable Cu^+-iodoalkyne complex) as energetic reference state.

Computational methods

The performance of several different functionals was initially tested and compared with MP2: B3LYP[31–33], BHHLYP (50% HF exchange + plus 50% B88[34] exchange, with LYP correlation), B3PW91[31,35], PBEPW91[35,36], PBE0[37] , PBE1PW91[35,36], and X3LYP[38]. All geometry optimizations were performed with the Firefly[39] quantum chemistry package, which is partially based on the GAMESS (US)[40] code, using autogenerated delocalized coordinates[41]. The SBKJ pseudo-potential[42] (and associated basis set) was used for Cu and I, and a medium-sized basis set, 6-31G(d), for all other elements. IRC computations confirmed that the obtained transition states did connect the relevant reactant and product states. Zero-point and thermal effects on the free energies at 298.15 K were computed at the optimized geometries. DFT energies of the optimized geometries obtained with each density functional were then computed using the same functional using 6-311G(2d,p) for all elements except Cu, which used the s6-31G* basis set developed by Swart *et al.*[43]. As before, the SBKJ pseudo-potential was used to describe the core electrons of Cu and I. MP2 single-point energies were extrapolated to the complete basis set limit using the method described by Zhao and Truhlar[44]. Unless otherwise noted, all energy values described in the text include solvation effects in tetrahydrofuran (ε=7.6) computed using the Polarizable Continuum Model[45–47] implemented in Firefly, as well as dispersion and repulsion interactions with the continuum solvent, which were computed using the Method developed by Amovili and Mennucci[48]. Cu^+-stabilization energies of reactants and transition states (Tables 5 and 7) were computed as the difference between the energies of Cu^+-complexed reactant (or transition states) and infinitely-separated reactant (or transition state) and $Cu^+(NH_3)_2$.

Intra- and inter-molecular dispersion effects were computed with the DFT-D3 formalism developed by Grimme et al.[49]. DFT-D3 parameters for PBEPW91 and PBE1PW91 were taken from our previous work[50]. The electrophilicity index (ω)[51] and nucleophilicity N index[52] were computed using the

HOMO/LUMO energies as approximations to the ionization potential and electron affinity. Global electron density transfer (GEDT)[53] was computed on every transition state using charges derived from Natural Population Analysis[54]. Dual descriptor[55] and condensed Fukui functions[56] (or condensed dual descriptors) using Hirshfeld[57] charges were computed and displayed using Multiwfn3.6[58].

Due to the experimental and computational results which rule out the proposals involving σ-bond formation between Cu^+ and iodoalkynes, we have focused our attention on the possible mechanisms involving π-complexation of the iodoalkyne (Figure 2). For each possible product (5-iodotriazole or 4-iodotriazole), we analyzed mechanisms involving the attack of the halogenated carbon or the substituted alkyne carbon by Cu^+-complexed azide , as well as the single-step reaction of azide with Cu^+-complexed iodoalkyne. Reaction mechanisms were computed for twenty-four different combinations of iodoalkynes and azides to explore the influence of electron-withdrawing (which are seldom used in the experimental reactants[28,59–61]) and electron-donating substituents as well as the presence of additional conjugation in the azide moiety. We tested six different azides (bearing either hydrogen or methyl, trifluoromethyl, phenyl, p-metylphenyl or p-nitrophenyl substituents) and four iodoalkynes (bearing trifluoromethyl, methyl, ethyl or phenyl groups). The large number of geometry optimizations required for the analysis of six pathways and twenty-four reactant combinations led us to choose ammonia as Cu^+-ligand instead of more efficient, yet prohibitively larger, nitrogen bases (such as TBTA or TTTA[28]) to decrease computational cost. Vibrational analyses of all transitions states showed the presence of the expected imaginary frequency corresponding to the vibration connecting the reactant and the product state. No counter-ion was included, since our computations (Supporting Information) showed that in THF solution CuI readily reacts with two ammonia molecules and loses I^- to the bulk. This reaction is exergonic by 16 $kcal.mol^{-1}$ and proceeds with a small barrier (< 8 $kcal.mol^{-1}$).

Results

Earlier work has shown that the PBE family of functionals (specifically PBE0 and PBE1PW91) usually affords the best agreement with MP2 and CCSD(T) computations on the energetic and geometric characterization of Cu^+-iodoalkyne complexes[62]. An additional benchmarking study for the single-step addition of azide to 1-iodopropyne (Table 1 and Supporting Information) confirmed the suitability of the PBE family of functionals and showed that PBEPW91, which agreed within 1 $kcal.mol^{-1}$ with the MP2 activation energy, would be the best choice for a thorough DFT-based exploration of the potential energy surface of this reaction. The inclusion of dispersion effects through Grimme's D3 formalism improved the performance of most functionals but did not afford a better agreement of PBEPW91 with the reference

MP2 computations. All reaction mechanisms described in this work were therefore studied using plain PBEPW91.

Conceptual DFT descriptors of six azides (hydrogen azide, methyl azide, phenyl azide, trifluoromethyl azide, *p*-nitrophenyl azide and *p*-methylphenylazide) and four iodoalkynes (bearing methyl, ethyl, trifluoromethyl or phenyl substituents), either free or complexed to $Cu^{+}(NH_3)_2$, are detailed in Table 2. The electrophilicity of iodoalkynes is quite insensitive to the identity of their substituents, whereas that of azides is strongly increased by the presence of electron-withdrawing substituents. Complexation with $Cu^{+}(NH_3)_2$ strongly increases the electrophilicity of the iodoalkynes and slightly decreases their nucleophilicities. The existence, for most iodoalkynes, of azides with either higher or lower electrophilicities suggests that the iodoalkynes might be acting as electron-donors towards some azides and as electron-acceptors towards others. Analysis of the dual descriptors (Supporting Information), however, shows this not to be the case: in iodoalkynes, only the negative portion of the dual descriptor (corresponding to the nucleophilic portions) is geometrically accessible (as it lies along the C-C π bond), whereas in the azides each nitrogen atom bears both negative and positive portions of the dual descriptor (in orthogonal orientations), enabling them to act as electrophiles towards the iodoalkynes when properly oriented. The presence of positive and negative portions of the dual descriptor on the same molecular centers further prevented the computation of condensed dual descriptors or condensed Fukui functions from providing additional clarity and insight. Overall, conceptual DFT descriptors were found insufficient to account for the experimental regioselectivity or to detect reactivity trends.

The uncatalyzed cycloadditions of the six azides with each of the four iodoalkynes were studied first. The activation energies range from 21.1 kcal.mol^{-1} (addition of methyl azide to I-C≡C-CF_3) to 28.3 kcal.mol^{-1} (addition of phenylazide to iodo(ethynylbenzene)), with no clear preference for the formation of one of the products relative to the other (Table 3). The electron-withdrawing effect of the trifluoromethyl group on the alkyne bond consistently afforded the lowest-energy transition states (and hence higher predicted reaction rates), except for the reaction with trifluoromethyl azide, where iodoalkynes bearing electron-donating substituents performed better. Inclusion of an aromatic substituent in the iodoalkyne yielded modest changes relative to the reference 1-iodopropyne except in the reactions with azides bearing aromatic substituents, which became slower. Analysis of the global electron density transfer revealed these transition states to be of non-polar character (GEDT<0.15). No correlation was found between the degree of electron density transfer and the activation energies.

Although the reaction occurs in all instances through a single-step mechanism where both carbon-nitrogen bonds are formed simultaneously, the transition state is rather assymetrical:e.g. in the transition states for the synthesis of 4-iodotriazoles (Figure 4A and Supporting Information), the C-N distances involving the iodinated alkyne carbon/azide terminal nitrogen are generally 0.15-0.50 Å shorter than the C-N distances

involving the other alkyne carbon. Significant differences in C-N bond lengths are also found in the transition states for the formation of 5-iodotriazoles from aromatic iodoalkynes or azides bearing electron-withdrawing trifluoromethyl groups or aromatic substituents, where the C-N bond to the halogenated carbon is up to 0.3 Å longer than the C-N bond between the non-halogenated carbon and the azide terminal nitrogen atom. In contrast, the two C-N bonds in the transition state of the synthesis of 5-iodotriazoles from methyl or hydrogen azide and non-aromatic iodoalkynes differ by less than 0.10 Å.

Other substituent effects on the transition state C-N distances are subtler. In the synthesis of 4-iodotriazoles (Figure 4A), presence of electron-withdrawing groups on the iodoalkyne leads to an elongation of the iodinated C-N distance and a dramatic shortening (up to 0.15 Å) of the C-N distance at the substituted alkyne carbon, and the presence of aromatic or electron-withdrawing substituents on the azide has the opposite effect. The transition state C-N distances are affected differently in the reaction leading to the 5-iodotriazoles (Figure 4B): electron-withdrawing or aromatic azide substituents now lead to an increase of C-N distance at the iodinated carbon (and a decrease in the other distance) and electron-withdrawing alkyne substituents no longer have any significant influence on those geometric parameters. Addition of aromaticity to the alkyne, however, now decreases the iodinated C-N distance and increases the distance between the substituted carbon and the azide.

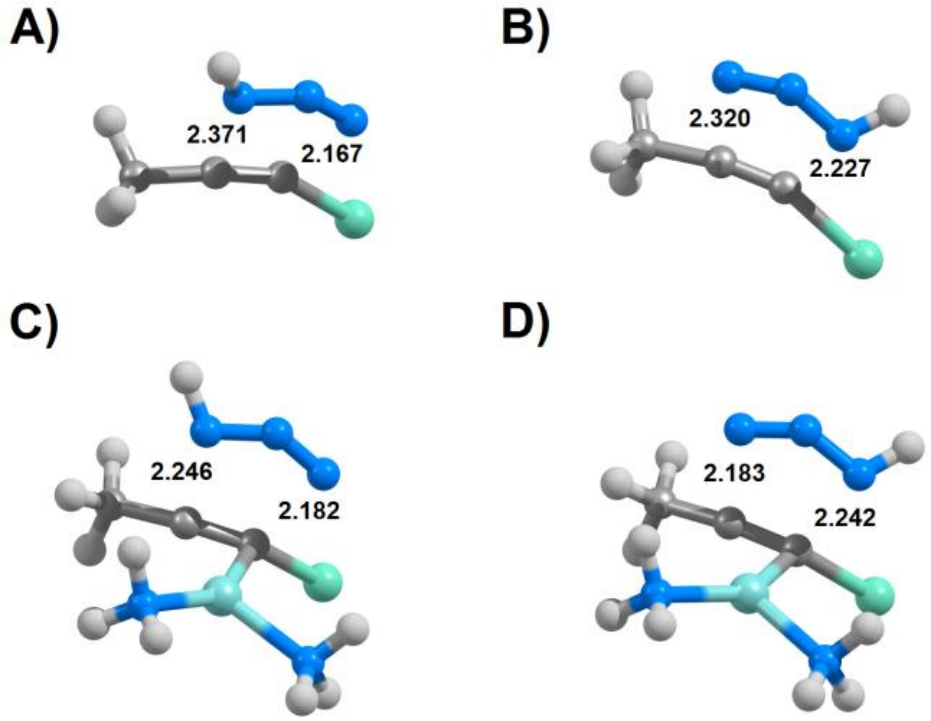

Figure 4: Transition states for the single-step addition of hydrogen azide to 1-iodopropyne computed at the PBEPW91 theory level. A) uncatalyzed formation of 4-iodotriazole; B) uncatalyzed formation of 5-

iodotriazole; C) Cu^{+}-catalyzed formation of 4-iodotriazole; D) Cu^{+}-catalyzed formation of 5-iodotriazole. Distances (in Å) between the reacting nitrogen and carbon atoms are shown.

A very similar single-step cycloaddition mechanism is possible under Cu^{+} catalysis (Figure 4, panels C and D): the C-C triple bond in the alkyne is first weakened by complexation with Cu^{+}, and azide addition then follows. The transition states of these reactions have shorter C-N distances than those of the corresponding un-catalyzed reactions, especially at the non-halogenated carbon, but the influence of the azide and alkyne substituents remains similar to the observed in the un-catalyzed reaction. A preference towards the formation of the 5-regioisomer is now observed, especially in the reactions with electron-deficient azides. As in the uncatalyzed reaction, analysis of the global electron density transfer revealed all transition states to be of non-polar (GEDT<0.15) or barely-polar character and no correlation was present between the degree of electron density transfer and the activation energies.

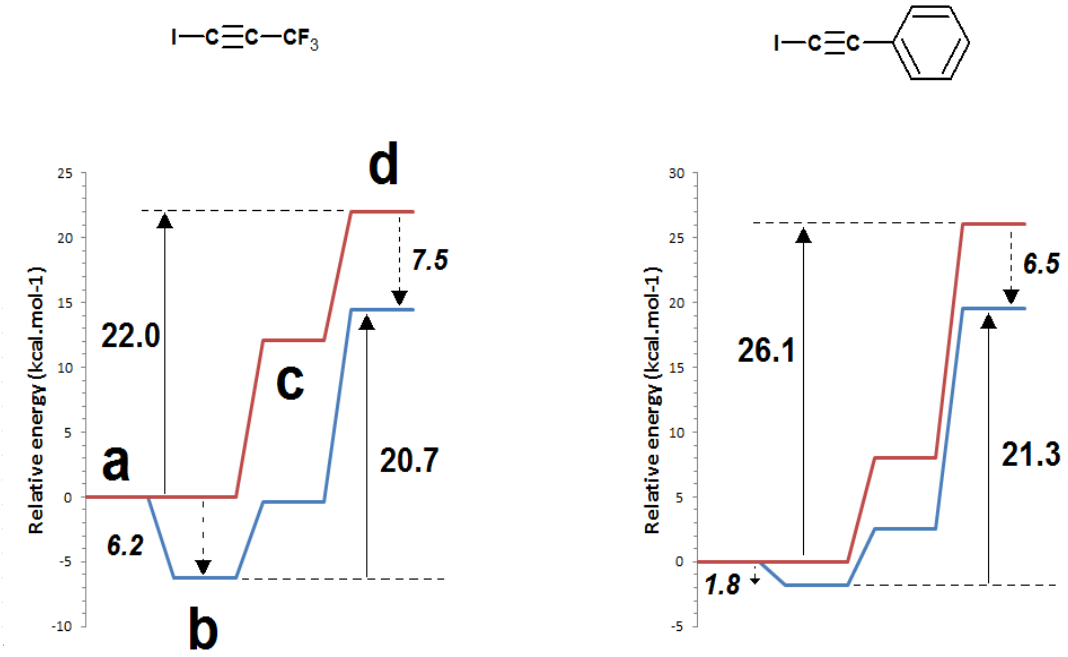

Figure 5: Potential Gibbs free energy surfaces for the single-step mechanism of 5-iodotriazole synthesis from hydrazoic acid and selected iodoalkynes in the catalyzed (blue) and uncatalyzed (red) states. a) infinitely-separated azide, alkyne and catalyst; b) catalyst-bound alkyne + infinitely separated azide; c) pre-reactional complex; d) transition state.

Relative to the infinitely separated reactants, the energy of the transition states is generally lowered in the Cu^{+}-catalyzed single-step reactions (Figure 3, mechanisms 1→4 and 1→5), but this lowering does not

entail an identical lowering of the activation energies for the reaction due to the exergonicity of the alkyne complexation by the catalyst (Figure 5 and Table 4). In several instances, the enhanced stability of the Cu^+-alkyne complex completely offsets the stabilizing effect of the catalyst on the transition state, leading to higher activation energies and therefore lower reaction rates for the single-step mechanisms in the presence of Cu^+ (Table 5).

Alternative mechanistic pathways involving binding of azide to the Cu^+ catalyst may arise from interactions between the metal and the substituent-bearing nitrogen atom (henceforth labelled as "the proximal nitrogen of the azide") or through the terminal nitrogen atom (which we label "the distal nitrogen of the azide"). Our computations show that such direct complexation is not possible for the strongly electron-deficient trifluoromethyl due to the lack of enough electron density in any of its nitrogen atoms. Methyl, phenyl, *p*-methylphenyl and *p*-nitrophenyl groups preferentially bind the Cu^+-catalyst through the distal nitrogen atom, whereas no preference is found in hydrogen azide (See supporting information). For these azides, Cu^+-complexation is endergonic by 3-12 kcal.mol^{-1}, in contrast to the 1.7-6.2 kcal.mol^{-1} exergonicity of the complexation of the iodoalkynes by the Cu^+ complexes, which entails that Cu^+-iodoalkyne complexes are overwhelmingly more likely to be formed than Cu^+-azide complexes when sub-stoichiometric amounts of catalyst are used. Putative reaction mechanisms involving Cu^+-azide complexes and uncomplexed iodoalkynes are therefore exceedingly unfavoured and were not studied further. Pathways involving azide binding to the previously-formed Cu^+-iodoalkyne complex (either prior to, or simultaneous with the formation of a C-N bond) remain nevertheless a possibility, as the ensuing electronic redistribution could plausibly affect the reactivity of the opposite terminal of the azide and its ability to attack the iodoalkyne (Figure 3, pathways 1→3→4 , 1→3→5, 1→2→4 and 1→2→5).

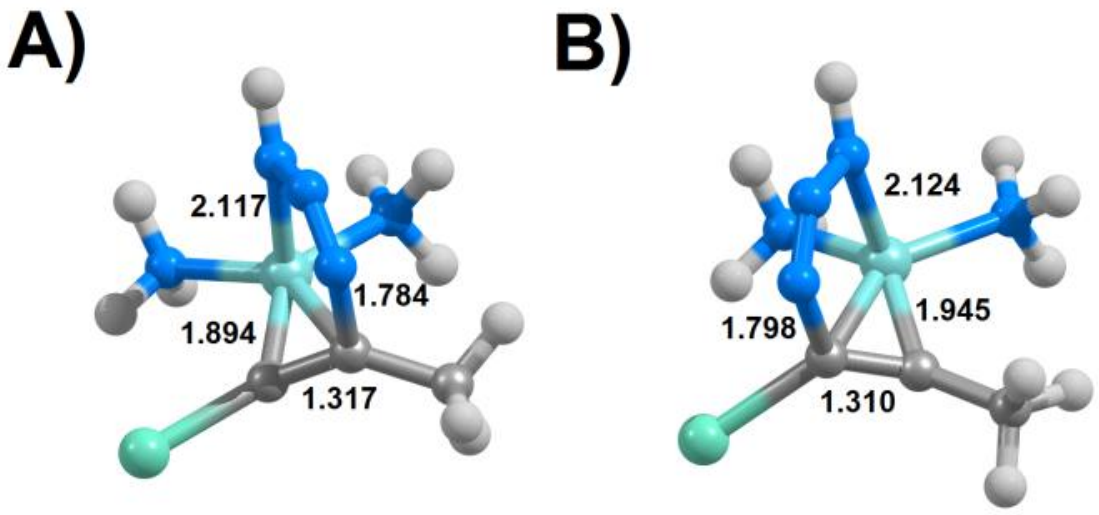

Figure 6: Transition states for the reaction of Cu^{+}-complexed 1-iodopropyne with the **distal** nitrogen atom of Cu^{+}-bound azide, computed at the PBEPW91 theory level. A) synthesis of 5-iodotriazole; B) synthesis of 4-iodotriazole

The reaction regioselectivity of the 1→3→4 and 1→3→5 pathways is determined by the relative ease of reaction of each of the alkyne carbon atoms with the azide distal nitrogen atom: 4-iodotriazoles arise from preferential reaction with the iodinated carbon atom, whereas 5-iodotriazoles form when the other carbon atom is more susceptible (Figure 6). The length of the nascent C-N bond in these transition states is tuned by the alkyne substituent (increased by 0.07 to 0.10 Å by a phenyl group and slightly shortened by CF_3) and relatively insensitive to the nature of the azide substituents (especially for the synthesis of 5-iodotriazoles). For most azide/iodoalkyne combinations (Table 6), this mechanism preferentially affords the 5-iodotriazole product. This preference is only inverted for the reaction of 1-iodoethynylbenzene with non-aromatic azides, and for the reaction of the ethyl-substituted alkyne with the *p*-methylphenyl azide. Compared to the values obtained in the single-step pathway, the presence of an electron-withdrawing CF_3 group on the alkyne strongly hampers the reactivity at both ends of the C-C triple bond in all but one case. This effect is stronger on the opposite end of the C-C triple bond (i.e. on the iodinated carbon), leading to activation energies in excess of 27 $kcal.mol^{-1}$. The exception to this trend is observed in the reaction between the non-halogenated carbon of CF_3-substituted iodoalkyne with trifluoromethylazide, which has a lower activation energy than the corresponding single-step reaction. Aromatic or electron-poor azides generally prefer this pathway (over the single-step one) when reacting with aromatic or electron-rich iodoalkynes. Hydrogen azide and methyl azide tend to prefer the single-step pathway.

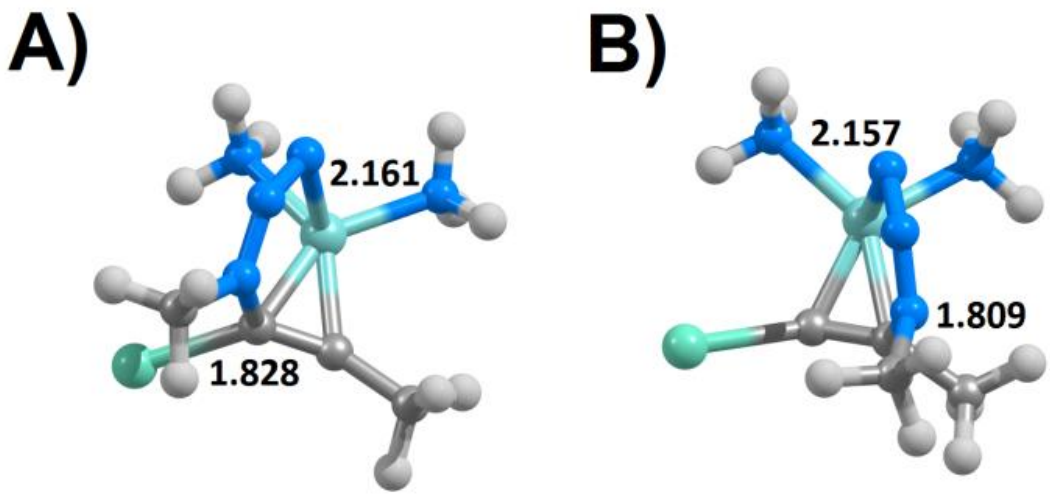

Figure 7: Transition states for the attack of Cu^{+}-complexed 1-iodopropyne by the **proximal** nitrogen atom of Cu^{+}-bound methyl azide, computed at the PBEPW91 theory level. A) synthesis of 5-iodotriazole; B) synthesis of 4-iodotriazole

Complexation of the Cu^{+}-iodoalkyne by the electron-rich distal nitrogen atom of azide (Figure 3, pathways 1→2→4 , 1→2→5), followed by attack of the azide proximal nitrogen atom by the the triple bond afforded the least convenient pathway for all azide/iodoalkyne combinations tested (Table 8), with activation energies up to 12 $kcal.mol^{-1}$ above those observed in the absence of catalyst. This "anti-catalytic" effect increases with the size of the azide substituent and is usually more intense for the formation of the 5-iodotriazole than the 4-iodotriazole, which suggests that it is partly due to steric clashes between the azide substituent and the iodine atom (Figure 7), which also tend to favour the formation of the 4-iodotriazole instead of the 5-iodotriazole. Trifluoromethyl azide reacts exceedingly slowly, as expected from the decreased electronic population on its proximal nitrogen atom due to the presence of a strong electron-withdrawing group.

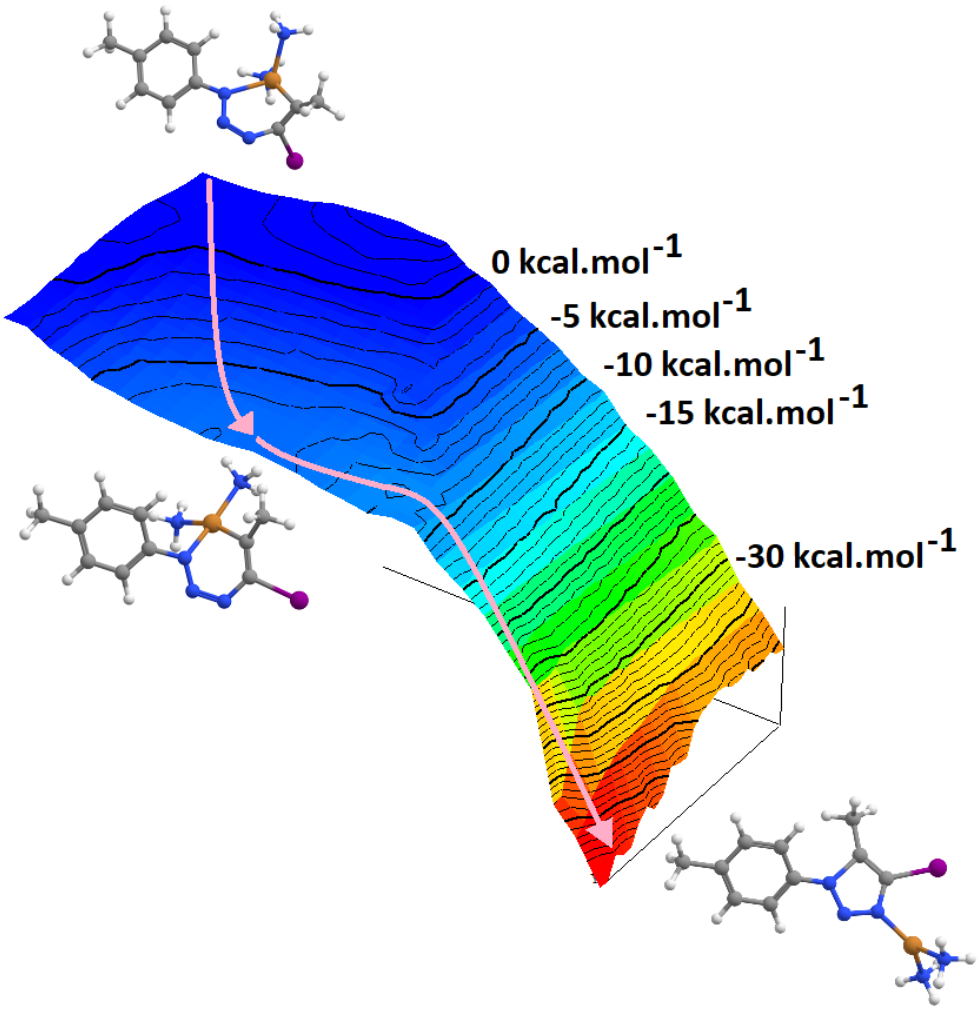

Figure 8: Potential energy surface of the conversion of the Cu^{+}-containing 6-membered ring intermediate into triazole.

The transition states depicted in figures 6 and 7 yield Cu-containing 6-membered rings, which have been shown by Lal et al.[30] in their study of the reaction between benzyl azide and 1-iodo(ethynylbenzene), to be "hidden intermediates", as the barriers for their conversion into separated catalyst and triazole products is negligible. Our efforts to characterize the conversion of these hidden intermediates into products through two-dimensional geometry scans (Figure 8) encountered transition state candidate structures with energies within 2 $kcal.mol^{-1}$ of the hidden intermediates in the first azide/iodoalkyne combination tested, showing that the conversion of the Cu-containing 6-membered rings into products does not encounter any relevant barrier. We therefore did not expend additional efforts in the characterization of those low-lying transition state candidates.

Discussion

The choice of reaction mechanism in the presence of Cu^+ catalyst is strongly affected by the iodoalkyne and azide substituents. Although the computational accuracy of DFT-computed barriers does not allow the discrimination of mechanisms differing by much more than 1 kcal.mol^{-1}, analysis of the data in Tables 3-8 shows that for most azide/iodoalkyne combinations one of the reaction pathways is clearly favoured. With an electron-withdrawing group on the alkyne, the single-step reaction mechanism is favoured in almost all cases regardless of the nature of the azide. Methyl azide follows the same single-step mechanism regardless of the nature of the iodoalkyne, except in the synthesis of the 5-regioisomer with the ethyl-substitued iodoalkyne. Aromatic azides, in contrast, generally bind the iodoalkyne-complexed Cu^+ ion using their proximal nitrogen atoms and then react with the iodoalkyne using their distal nitrogens (unless the iodoalkyne is severely electron-deficient, in which case they follow the single-step pathway). Hydrogen azide follows a single-step pathway when forming 4-iodotriazoles, and formation of 5-iodotriazoles from electron-rich alkynes requires azide binding to the iodoalkyne-bound copper. In only two instances (the reactions of hydrogen azide and trifluoromethylazide with 1-iodoethenylbenzene) was the formation of the 4-iodotriazole predicted to be clearly favoured over the commonly observed 5-iodotriazole. The catalytic gain is heavily dependent on the substituents, as the computed activation energy decrease ranges between 0.1 – 7.0 kcal.mol^{-1}. The highest catalytic effects are observed with aromatic iodoalkynes or electron-deficient azides.

The catalytic effect of the Cu^+-complex arises from a delicate balance of effects, as the initial exergonic formation of the π-complex contributes to a barrier increase which may not always be compensated by the transition-state stabilization (Tables 5 and 7). Indeed, for the trifluoromethylated iodoalkyne, the reactant stabilization upon complexation makes all reaction pathways towards aromatic azides less favourable than observed in the absence of copper(I). This observation may explain the relative fastidiousness of this reaction relative to the nature of the bases used as coordinating ligands for Cu^+, since it entails that only those ligands which stabilize the transition state more than they enhance the alkyne-complexation ability of Cu^+ can be used as suitable catalysts. The possibility of saturation of the Cu^+ coordination sphere by the ligands further complicates the choice of suitable coordinating ligand: for example, no reaction takes place in the presence of phenantroline[28], and we have been able to determine (Supporting Information) that this inhibition is due to the very exergonic (-36 kcal.mol^{-1}) formation of $Cu^+(phen)_2$, which contains a saturated coordination sphere and can therefore no longer activate

alkyne bonds. Phenantroline can however be used as a copper ligand in the cycloaddition of azides to terminal alkynes[13] because the initial deprotonation of the alkyne yields an anion with much higher coordination ability than the triple bond of iodoalkyne, and therefore competes with other ligands for Cu^+ coordination.

Conclusions

The Cu^+-catalyzed reaction of iodoalkynes with azides proceeds through an initial complexation of the iodoalkyne by the metal. Subsequent steps depend on the nature of the iodoalkyne and azide species: electron-deficient iodoalkynes react with azides through a single-step mechanism where both C-N bonds are formed simultaneously, but in other cases both C-N bonds will be formed sequentially, through azide binding to Cu^+ through its proximal nitrogen, followed by attack of the non-halogenated alkyne carbon by the distal nitrogen atom. The catalytic gain obtained through the use of Cu^+ depends only partially on its direct effect on the energy of the transition state (relative to that of the infinitely separated reactants) and may be lost if the iodoalkyne itself strongly interacts with the catalyst through the formation of too strong a π-complex.

Author's contributions

C.E.P.B. and P.J.S. jointly performed the computations and analysed the results. P.J.S. further conceived and designed the study, and wrote the manuscript.

Acknowledgements

This work has been financed by FEDER through Programa Operacional Factores de Competitividade – COMPETE and by Portuguese Funds through FCT – Fundação para a Ciência e a Tecnologia under project PTDC/QUI-QUI/111288/2009.

Conflicts of interest

There are no conflicts of interest to declare

Supporting Information

Coordinates of all molecules described in the text, as well as individual energetic data. Full inputs and output files may be downloaded from figshare (DOI: 10.6084/m9.figshare.5165878 ,

10.6084/m9.figshare.5035682 , 10.6084/m9.figshare.5418688 , 10.6084/m9.figshare.5459674 , 10.6084/m9.figshare.5478751)

References

(1) Kolb, H. C.; Finn, M. G.; Sharpless, K. B. Click Chemistry: Diverse Chemical Function from a Few Good Reactions. *Angew. Chem. Int. Ed. Engl.* **2001**, *40* (11), 2004–2021.

(2) Huisgen, R. 1,3-Dipolar Cycloadditions. Past and Future. *Angew. Chemie Int. Ed. English* **1963**, *2* (10), 565–598.

(3) Hein, C. D.; Liu, X.-M.; Wang, D. Click Chemistry, A Powerful Tool for Pharmaceutical Sciences. *Pharm. Res.* **2008**, *25* (10), 2216–2230.

(4) Kolb, H. C.; Sharpless, K. B. The Growing Impact of Click Chemistry on Drug Discovery. *Drug Discov. Today* **2003**, *8* (24), 1128–1137.

(5) Kühle, E. One Hundred Years of Sulfenic Acid Chemistry II A. Oxidation, Reduction, and Addition Reactions of Sulfenyl Halides 1. *Synthesis (Stuttg).* **1971**, No. 11, 563–586.

(6) Adolfsson, H.; Converso, A.; Sharpless, K. B. Comparison of Amine Additives Most Effective in the New Methyltrioxorhenium-Catalyzed Epoxidation Process. *Tetrahedron Lett.* **1999**, *40* (21), 3991–3994.

(7) Kolb, H. C.; VanNieuwenhze, M. S.; Sharpless, K. B. Catalytic Asymmetric Dihydroxylation. *Chem. Rev.* **1994**, *94* (8), 2483–2547.

(8) Gontcharov, A. V.; Liu, H.; Sharpless, K. B. Tert -Butylsulfonamide. A New Nitrogen Source for Catalytic Aminohydroxylation and Aziridination of Olefins. *Org. Lett.* **1999**, *1* (5), 783–786.

(9) Lundberg, P.; Hawker, C. J.; Hult, A.; Malkoch, M. Click Assisted One-Pot Multi-Step Reactions in Polymer Science: Accelerated Synthetic Protocols. *Macromol. Rapid Commun.* **2008**, *29* (12–13), 998–1015.

(10) Rostovtsev, V. V; Green, L. G.; Fokin, V. V; Sharpless, K. B. A Stepwise Huisgen Cycloaddition Process: Copper(I)-Catalyzed Regioselective Ligation of Azides and Terminal Alkynes. *Angew. Chemie Int. Ed.* **2002**, *41* (14), 2596–2599.

(11) Tornøe, C. W.; Meldal, M. Peptidotriazoles: Copper (I)-Catalyzed 1, 3-Dipolar Cycloadditions on Solid-Phase. In *Peptides-American Symposium*; 2001; Vol. 17, pp 263–264.

(12) Tornøe, C. W.; Christensen, C.; Meldal, M. Peptidotriazoles on Solid Phase: [1,2,3]-Triazoles by Regiospecific copper(I)-Catalyzed 1,3-Dipolar Cycloadditions of Terminal Alkynes to Azides. *J. Org. Chem.* **2002**, *67* (9), 3057–3064.

(13) Himo, F.; Lovell, T.; Hilgraf, R.; Rostovtsev, V. V; Noodleman, L.; Sharpless, K. B.; Fokin, V. V.

Copper(I)-Catalyzed Synthesis of Azoles. DFT Study Predicts Unprecedented Reactivity and Intermediates. *J. Am. Chem. Soc.* **2005**, *127* (1), 210–216.

(14) Iacobucci, C.; Reale, S.; Gal, J.-F.; De Angelis, F. Dinuclear Copper Intermediates in Copper(I)-Catalyzed Azide-Alkyne Cycloaddition Directly Observed by Electrospray Ionization Mass Spectrometry. *Angew. Chemie Int. Ed.* **2015**, *54* (10), 3065–3068.

(15) Özkılıç, Y.; Tüzün, N. S. A DFT Study on the Binuclear CuAAC Reaction: Mechanism in Light of New Experiments. *Organometallics* **2016**, *35* (16), 2589–2599.

(16) Buckley, B. R.; Dann, S. E.; Heaney, H. Experimental Evidence for the Involvement of Dinuclear Alkynylcopper(I) Complexes in Alkyne-Azide Chemistry. *Chem. - A Eur. J.* **2010**, *16* (21), 6278–6284.

(17) Ahlquist, M.; Fokin, V. V. Enhanced Reactivity of Dinuclear Copper(I) Acetylides in Dipolar Cycloadditions. *Organometallics* **2007**, *26* (18), 4389–4391.

(18) Worrell, B. T.; Malik, J. A.; Fokin, V. V. Direct Evidence of a Dinuclear Copper Intermediate in Cu(I)-Catalyzed Azide-Alkyne Cycloadditions. *Science (80-.).* **2013**, *340* (6131), 457–460.

(19) Calvo-Losada, S.; Pino-González, M. S.; Quirante, J. J. Rationalizing the Catalytic Activity of Copper in the Cycloaddition of Azide and Alkynes (CuAAC) with the Topology of $\nabla 2 \rho(R)$ and $\nabla\nabla 2 \rho(R)$. *J. Phys. Chem. B* **2015**, *119*, 1243–1258.

(20) Nolte, C.; Mayer, P.; Straub, B. F. Isolation of a copper(I) Triazolide: A “click” intermediate. *Angew. Chem. Int. Ed. Engl.* **2007**, *46* (12), 2101–2103.

(21) Berg, R.; Straub, B. F. Advancements in the Mechanistic Understanding of the Copper-Catalyzed Azide-Alkyne Cycloaddition. *Beilstein J. Org. Chem.* **2013**, *9*, 2715–2750.

(22) Straub, B. F. Mu-Acetylide and Mu-Alkenylidene Ligands In “click” triazole Syntheses. *Chem. Commun. (Camb).* **2007**, 3868–3870.

(23) Jin, L.; Tolentino, D. R.; Melaimi, M.; Bertrand, G. Isolation of Bis(copper) Key Intermediates in Cu-Catalyzed Azide-Alkyne Click Reaction. *Sci. Adv.* **2015**, *1* (June), 1–5.

(24) Buckley, B. R.; Heaney, H. Mechanistic Investigations of Copper(I)-Catalysed Alkyne–Azide Cycloaddition Reactions. In *Topics in Heterocyclic Chemistry*; 2012; Vol. 28, pp 1–29.

(25) Zhu, L.; Brassard, C. J.; Zhang, X.; Guha, P. M.; Clark, R. J. On the Mechanism of Copper(I)-Catalyzed Azide–Alkyne Cycloaddition. *Chem. Rec.* **2016**, No. I, 1501–1517.

(26) Rodionov, V. O.; Fokin, V. V.; Finn, M. G. Mechanism of the Ligand-Free CuI-Catalyzed Azide-Alkyne Cycloaddition Reaction. *Angew. Chemie Int. Ed.* **2005**, *44* (15), 2210–2215.

(27) Rodionov, V. O.; Presolski, S. I.; Díaz Díaz, D.; Fokin, V. V.; Finn, M. G. Ligand-Accelerated Cu-Catalyzed Azide−Alkyne Cycloaddition: A Mechanistic Report. *J. Am. Chem. Soc.* **2007**, *129* (42), 12705–12712.

(28) Hein, J. E.; Tripp, J. C.; Krasnova, L. B.; Sharpless, K. B.; Fokin, V. V. Copper(I)-Catalyzed Cycloaddition of Organic Azides and 1-Iodoalkynes. *Angew. Chem. Int. Ed. Engl.* **2009**, *48* (43), 8018–8021.

(29) Barsoum, D. N.; Okashah, N.; Zhang, X.; Zhu, L. Mechanism of Copper(I)-Catalyzed 5-Iodo-1,2,3-Triazole Formation from Azide and Terminal Alkyne. *J. Org. Chem.* **2015**, *80* (19), 9542–9551.

(30) Lal, S.; Rzepa, H. S.; Díez-González, S. Catalytic and Computational Studies of N-Heterocyclic Carbene or Phosphine-Containing Copper(I) Complexes for the Synthesis of 5-Iodo-1,2,3-Triazoles. *ACS Catal.* **2014**, *4* (7), 2274–2287.

(31) Becke, A. D. Density-Functional Thermochemistry. III. The Role of Exact Exchange. *J. Chem. Phys.* **1993**, *98* (7), 5648–5652.

(32) Lee, C.; Yang, W.; Parr, R. G. Development of the Colle-Salvetti Correlation-Energy Formula into a Functional of the Electron Density. *Phys. Rev. B* **1988**, *37* (2), 785–789.

(33) Hertwig, R. H.; Koch, W. On the Accuracy of Density Functionals and Their Basis Set Dependence: An Extensive Study on the Main Group Homonuclear Diatomic Molecules Li2 to Br2. *J. Comput. Chem.* **1995**, *16* (5), 576–585.

(34) Becke, A. D. Density-Functional Exchange-Energy Approximation with Correct Asymptotic Behavior. *Phys. Rev. A* **1988**, *38* (6), 3098–3100.

(35) Perdew, J. P. Unified Theory of Exchange and Correlation beyond the Local Density Approximation. In *Electronic Structure of Solids '91*; Ziesche, P., Eschrig, H., Eds.; Physical Research; Akademie Verlag: Berlin, 1991; Vol. 17, pp 11–20.

(36) Perdew, J. P.; Burke, K.; Ernzerhof, M. Generalized Gradient Approximation Made Simple. *Phys. Rev. Lett.* **1996**, *77*, 3865–3868.

(37) Adamo, C.; Barone, V. Toward Reliable Density Functional Methods without Adjustable Parameters: The PBE0 Model. *J. Chem. Phys.* **1999**, *110* (1999), 6158.

(38) Xu, X.; Zhang, Q.; Muller, R. P.; Goddard, W. A. An Extended Hybrid Density Functional (X3LYP) with Improved Descriptions of Nonbond Interactions and Thermodynamic Properties of Molecular Systems. *J. Chem. Phys.* **2005**, *122* (1), 14105.

(39) Granovsky, A. A. Firefly 8.0.0. 2013.

(40) Schmidt, M. W.; Baldridge, K. K.; Boatz, J. A.; Elbert, S. T.; Gordon, M. S.; Jensen, J. H.; Koseki, S.; Matsunaga, N.; Nguyen, K. A.; Su, S.; et al. General Atomic and Molecular Electronic Structure System. *J. Comput. Chem.* **1993**, *14* (11), 1347–1363.

(41) Baker, J.; Kessi, A.; Delley, B. The Generation and Use of Delocalized Internal Coordinates in Geometry Optimization. *J. Chem. Phys.* **1996**, *105*, 192–212.

(42) Stevens, W. J. W.; Krauss, M.; Basch, H.; Jasien, P. G. Relativistic Compact Effective Potentials

and Efficient, Shared-Exponent Basis Sets for the Third-, Fourth-, and Fifth-Row Atoms. *Can. J. …* **1992**, *70* (6), 612–630.

(43) Swart, M.; Güell, M.; Luis, J. M.; Solà, M. Spin-State-Corrected Gaussian-Type Orbital Basis Sets. *J. Phys. Chem. A* **2010**, *114* (26), 7191–7197.

(44) Zhao, Y.; Truhlar, D. G. Infinite-Basis Calculations of Binding Energies for the Hydrogen Bonded and Stacked Tetramers of Formic Acid and Formamide and Their Use for Validation of Hybrid DFT and Ab Initio Methods. *J. Phys. Chem. A* **2005**, *109*, 6624–6627.

(45) Tomasi, J.; Persico, M. Molecular Interactions in Solution: An Overview of Methods Based on Continuous Distributions of the Solvent. *Chem. Rev.* **1994**, *94* (7), 2027–2094.

(46) Mennucci, B.; Tomasi, J. Continuum Solvation Models: A New Approach to the Problem of Solute's Charge Distribution and Cavity Boundaries. *J. Chem. Phys.* **1997**, *106* (12), 5151–5158.

(47) Cossi, M.; Mennucci, B.; Pitarch, J.; Tomasi, J. Correction of Cavity-Induced Errors in Polarization Charges of Continuum Solvation Models. *J. Comput. Chem.* **1998**, *19* (8), 833–846.

(48) Amovilli, C.; Mennucci, B. Self-Consistent-Field Calculation of Pauli Repulsion and Dispersion Contributions to the Solvation Free Energy in the Polarizable Continuum Model. *J. Phys. Chem. B* **1997**, *5647* (96), 1051–1057.

(49) Grimme, S.; Antony, J.; Ehrlich, S.; Krieg, H. A Consistent and Accurate Ab Initio Parametrization of Density Functional Dispersion Correction (DFT-D) for the 94 Elements H-Pu. *J. Chem. Phys.* **2010**, *132* (15), 154104.

(50) Bernardo, C. E. P.; Silva, P. J. Computational Exploration of the Reaction Mechanism of the Cu + -Catalysed Synthesis of Indoles from N -Aryl Enaminones. *R. Soc. Open Sci.* **2016**, *3* (2), 150582.

(51) Parr, R. G.; Szentpály, L. v.; Liu, S. Electrophilicity Index. *J. Am. Chem. Soc.* **1999**, *121* (9), 1922–1924.

(52) Domingo, L. R.; Chamorro, E.; Pérez, P. Understanding the Reactivity of Captodative Ethylenes in Polar Cycloaddition Reactions. A Theoretical Study. *J. Org. Chem.* **2008**, *73* (12), 4615–4624.

(53) Domingo, L. R.; Sáez, J. A. Understanding the Mechanism of Polar Diels-Alder Reactions. *Org. Biomol. Chem.* **2009**, *7* (17), 3576–3583.

(54) Reed, A. E.; Weinstock, R. B.; Weinhold, F. Natural Population Analysis. *J. Chem. Phys.* **1985**, *83* (2), 735–746.

(55) Morell, C.; Grand, A.; Toro-Labbé, A. New Dual Descriptor for Chemical Reactivity. *J. Phys. Chem. A* **2005**, *109* (1), 205–212.

(56) Yang, W.; Mortier, W. J. The Use of Global and Local Molecular Parameters for the Analysis of the Gas-Phase Basicity of Amines. *J. Am. Chem. Soc.* **1986**, *108* (19), 5708–5711.

(57) Hirshfeld, F. L. Bonded-Atom Fragments for Describing Molecular Charge Densities. *Theor. Chim.*

Acta **1977**, *44* (2), 129–138.

(58) Lu, T.; Chen, F. Multiwfn: A Multifunctional Wavefunction Analyzer. *J. Comput. Chem.* **2012**, *33* (5), 580–592.

(59) García-Álvarez, J.; Díez, J.; Gimeno, J.; Suárez, F. J.; Vincent, C. (Iminophosphorane)copper(I) Complexes as Highly Efficient Catalysts for 1,3-Dipolar Cycloaddition of Azides with Terminal and 1-Iodoalkynes in Water: One-Pot Multi-Component Reaction from Alkynes and in Situ Generated Azides. *Eur. J. Inorg. Chem.* **2012**, *2012* (35), 5854–5863.

(60) García-Álvarez, J.; Díez, J.; Gimeno, J. A Highly Efficient Copper(i) Catalyst for the 1,3-Dipolar Cycloaddition of Azides with Terminal and 1-Iodoalkynes in Water: Regioselective Synthesis of 1,4-Disubstituted and 1,4,5-Trisubstituted 1,2,3-Triazoles. *Green Chem.* **2010**, *12* (12), 2127.

(61) Vidal, C.; García-Álvarez, J. Glycerol: A Biorenewable Solvent for Base-Free Cu(i)-Catalyzed 1,3-Dipolar Cycloaddition of Azides with Terminal and 1-Iodoalkynes. Highly Efficient Transformations and Catalyst Recycling. *Green Chem.* **2014**, *16* (7), 3515.

(62) Bernardo, C. E. P.; Bauman, N. P.; Piecuch, P.; Silva, P. J. Evaluation of Density Functional Methods on the Geometric and Energetic Descriptions of Species Involved in Cu^{+}-Promoted Catalysis. *J. Mol. Model.* **2013**, *19* (12), 5457–5467.

Table 1: Performance of selected density functionals vs. MP2 in the Cu^{+}(NH3)2-catayzed single-step addition of hydrogen azide (hydrazoic acid) to 1-iodopropyne. All energies are in kcal/mol, and were computed relative to the pre-reactional complex, rather than separated reactants. ZPVE and vibrational corrections to free energy have been included. Values in parentheses include dispersion effects computed with the –D3 methodology[49]. No dispersion correction was performed for X3LYP due to the lack of proper D3 parameters for this functional.

	Gas-phase activation free energy	Gas-phase reaction free energy	RMSD (Å) vs. MP2
B3LYP	28.2 (24.2)	-55.3 (-55.6)	0.148
B3PW91	26.3 (21.7)	-58.6 (-59.2)	0.141
BHHLYP	34.9 (31.7)	-66.3 (-66.9)	0.155
PBE0	24.9 (22.8)	-63.4 (-63.3)	0.128
PBE1PW91	25.2 (23.6)	-62.9 (62.3)	0.130
PBEPW91	19.5 (17.7)	-52.5 (-52.0)	0.116
X3LYP	27.8	-56.7	0.138
MP2	18.8	-48.6	0.000

Table 2: PPEPW91/6-311G(2d,p) electronic chemical potential (μ), electrophilicty(ω) and nucleophilicity (N), in eV, of azides, iodoalkynes, and Cu^{+}-complexed iodoalkynes.

	μ	ω	N
azide			
CF_3-N_3	-5.09	3.06	1.16
CH_3-N_3	-4.02	2.11	2.45
H-N_3	-4.22	2.12	2.05
Ph-N_3	-4.00	2.59	2.83
p-MePh-N_3	-3.90	2.59	3.00
p-NO_2Ph-N_3	-4.86	4.95	2.32
iodoalkyne			
CH_3-CC-I	-3.95	2.02	2.51
CH_3CH_2-CC-I	-3.92	2.01	2.54
CF_3-CC-I	-4.45	2.37	1.83
Ph-CC-I	-3.92	2.31	2.79
Cu^{+}-iodoalkyne			
CH_3-CC-I	-4.68	3.91	2.29
CH_3CH_2-CC-I	-4.68	3.91	2.30
CF_3-CC-I	-5.14	4.46	1.75
Ph-CC-I	-4.74	4.37	2.35

Table 3 Activation free energies for the catalyst-free single-step attack of iodoalkyne by azides, computed at the PBEPW91/6-311G(2d,p)$^{+}$s6-31G*//PBEPW91/6-31G(d)$^{+}$SBKJC theory level, in tetrahydrofuran. Iodoalkyne substituents are shown on the first column. The first energy in each pair refers to the formation of the 4-iodotriazole and the second refers to the formation of 5-iodotriazole. The most favorable energy in each pair is bolded, for ease of reference. All energies are in kcal/mol, and were computed relative to the separated azide and Cu^{+}-complexed iodoalkyne. ZPVE and vibrational corrections to free energy have been included.

Alkyne substituent	Azide substituent					
	H	CH_3	Ph	*p*-MePh	CF_3	*p*-NO_2Ph
CH_3	**25.0**/25.2	**24.6**/24.7	**24.6**/24.8	**24.6**/25.2	**22.3**/23.3	23.6/23.6
CF_3	22.1/**22.0**	21.5/**21.1**	22.8/**22.5**	23.1/**22.7**	24.8/**23.7**	23.5/**23.1**
CH_2CH_3	**25.1**/25.3	**24.9**/25.0	**24.9**/25.0	**24.6**/25.7	22.9/22.9	25.7/**24.3**
Ph	**25.8**/26.1	25.4/**25.1**	**27.8**/28.3	**25.4**/27.3	**25.2**/25.7	28.1/**26.7**

Table 4: Activation free energies for the single-step attack of Cu^{+}-iodoalkyne by azides, computed at the PBEPW91/6-311G(2d,p)$^{+}$s6-31G*//PBEPW91/6-31G(d)$^{+}$SBKJC theory level, in tetrahydrofuran. Iodoalkyne substituents are shown on the first column. The first energy in each pair refers to the formation of the 4-iodotriazole and the second refers to the formation of 5-iodotriazole. The most favorable energy in each pair is bolded, for ease of reference. All energies are in kcal/mol, and were computed relative to the separated azide and Cu^{+}-complexed iodoalkyne. ZPVE and vibrational corrections to free energy have been included.

Alkyne substituent	Azide substituent					
	H	CH_3	Ph	*p*-MePh	CF_3	*p*-NO_2Ph
CH_3	24.2/**23.9**	**23.2**/23.3	**26.8**/28.4	**26.6**/28.0	26.7/**25.5**	26.5/**25.4**
CF_3	21.4/**20.7**	22.6/**20.1**	**24.0**/24.3	23.8/**23.2**	26.7/**25.6**	25.7/**24.2**
CH_2CH_3	24.7/**24.2**	24.3/**24.1**	25.7/**25.6**	**25.0**/25.3	27.0/**25.2**	26.5/**24.6**
Ph	**19.5**/21.3	21.1/**20.7**	28.1/**24.0**	27.8/**24.2**	26.0/**22.8**	28.2/**24.7**

Table 5: Energetic influence of catalyst coordination on the alkynes and transition states of single-step cycloaddition of azides to iodoalkynes, computed at the PBEPW91/6-311G(2d,p)$^{+}$s6-31G*//PBEPW91/6-31G(d)$^{+}$SBKJC theory level, in tetrahydrofuran. Iodoalkyne substituents are shown on the first column. The first energy in each pair refers to the formation of the 4-iodotriazole and the second refers to the formation of 5-iodotriazole. Combinations where metal coordination stabilizes the isolated alkyne more than the transition state (and the reaction mechanism is therefore **slowed** by the Cu^{+}-complex) are bolded, for ease of reference. All stabilization energies are in kcal/mol. ZPVE and vibrational corrections to free energy have been included.

Alkyne substituent	Alkyne stabilization upon complexation	Transition state stabilization					
		H-N_3	CH_3-N_3	Ph-N_3	*p*-MePh-N_3	CF_3	*p*-NO_2Ph
CH_3	-4.1	-4.9/-5.4	-5.5/-5.4	**-1.9**/**-0.5**	**-2.1**/**-1.2**	**0.3**/**-1.9**	**-1.2**/**-2.2**
CF_3	-6.2	-6.9/-7.5	**-5.0**/-7.2	**-5.0**/**-4.4**	**-5.5**/**-5.8**	**-4.3**/**-4.3**	**-4.0**/**-5.1**
CH_2CH_3	-4.0	-4.4/-5.1	-4.7/-5.0	**-3.3**/**-3.4**	**-3.6**/-4.4	**0.0**/**-1.7**	**-3.2**/**-3.7**
Ph	-1.8	-8.1/-6.5	-6.1/-6.1	**-1.4**/-6.0	**0.6**/-5.0	**-0.9**/-4.6	-1.6/-**3.8**

Table 6: Activation free energies for the attack of Cu^{+}-iodoalkyne by the azide **distal** nitrogen, computed at the PBEPW91/6-311G(2d,p)$^{+}$s6-31G*//PBEPW91/6-31G(d)$^{+}$SBKJC theory level, in tetrahydrofuran. Iodoalkyne substituents are shown on the first column. The first energy in each pair refers to the formation of the 4-iodotriazole and the second refers to the formation of 5-iodotriazole. The most favorable energy in each pair is bolded, for ease of reference. All energies are in kcal/mol, and were computed relative to the separated azide and Cu^{+}-complexed iodoalkyne. ZPVE and vibrational corrections to free energy have been included.

Alkyne substituent	Azide substituent					
	H	CH_3	Ph	*p*-MePh	CF_3	*p*-NO_2Ph
CH_3	26.3/**22.2**	25.8/**25.5**	24.8/**23.9**	27.3/**23.8**	21.5/**18.3**	24.7/**23.2**
CF_3	30.1/**22.6**	30.6/**23.8**	30.7/**27.1**	27.0/**26.8**	32.4/**22.4**	30.7/**25.9**
CH_2CH_3	24.5/**19.1**	26.2/**23.5**	24.7/**23.3**	**24.5**/26.1	23.4/**21.1**	24.3/**23.7**
Ph	**21.7**/22.3	**22.8**/23.7	25.2/**24.3**	23.5/**23.0**	**18.1**/20.6	25.9/**23.8**

Table 7: Energetic influence of catalyst coordination on the alkynes and transition states of reaction of Cu^{+}-iodoalkyne with the azide **distal** nitrogen, computed at the PBEPW91/6-311G(2d,p)$^{+}$s6-31G*//PBEPW91/6-31G(d)$^{+}$SBKJC theory level, in tetrahydrofuran. Iodoalkyne substituents are shown on the first column. The first energy in each pair refers to the formation of the 4-iodotriazole and the second refers to the formation of 5-iodotriazole. Combinations where metal coordination stabilizes the isolated alkyne more than the transition state (and the reaction mechanism is therefore **slowed** by the Cu^{+}-complex) are bolded, for ease of reference. All stabilization energies are in kcal/mol. ZPVE and vibrational corrections to free energy have been included.

Alkyne substituent	Alkyne stabilization upon complexation	Transition state stabilization					
		H-N_3	CH_3-N_3	Ph-N_3	*p*-MePh-N_3	CF_3	*p*-NO_2Ph
CH_3	-4.1	**-2.8**/-7.1	**-2.9/-3.3**	**-3.9**/-5.0	**-1.4**/-5.5	-4.8/-8.1	**-3.0**/-4.5
CF_3	-6.2	**1.7/-5.6**	**2.9/-3.5**	**1.7/0.5**	**-2.3/-2.4**	**1.4**/-8.6	**1.1/-3.7**
CH_2CH_3	-4.0	-4.7/-10.2	**-2.7**/-5.6	-4.3/-5.7	-4.1/**-3.6**	**-3.5**/-5.8	-5.4/-6.0
Ph	-1.8	-5.9/-5.5	-4.4/-3.1	-4.4/-5.7	-3.7/-6.2	-8.8/-6.3	-3.9/-6.0

Table 8: Activation free energies for the attack of Cu^{+}-iodoalkyne by the azide **proximal** nitrogen, computed at the PBEPW91/6-311G(2d,p)$^{+}$s6-31G*//PBEPW91/6-31G(d)$^{+}$SBKJC theory level, in tetrahydrofuran. Iodoalkyne substituents are shown on the first column. The first energy in each pair refers to the formation of the 4-iodotriazole and the second refers to the formation of 5-iodotriazole. The most favorable energy in each pair is bolded, for ease of reference. All energies are in kcal/mol, and were computed relative to the separated azide and Cu^{+}-complexed iodoalkyne. ZPVE and vibrational corrections to free energy have been included.

Alkyne substituent	Azide substituent					
	H	CH_3	Ph	*p*-MePh	CF_3	*p*-NO_2Ph
CH_3	30.3/**30.2**	**29.3**/29.6	**32.9**/34.0	**33.5**/33.8	**32.8**/35.8	**33.1**/36.5
CF_3	**27.5**/31.2	**26.6**/29.6	**33.9**/36.0	**33.1**/34.7	**34.5**/38.7	**35.5**/37.5
CH_2CH_3	**29.0**/30.2	**28.6**/30.5	**35.4**/35.8	**32.8**/34.2	**31.9**/36.2	**32.6**/36.7
Ph	**26.9**/29.9	27.8/**26.8**	**31.2**/32.4	**30.2**/36.5	**30.7**/33.0	**31.1**/34.5